Asian Journal of Chemical Sciences

11(4): 8-22, 2022; Article no.AJOCS.88253
ISSN: 2456-7795

Synthesis, Characterization and Thermal Study of Some Transition Metal Complexes of N-(4-hydroxybenzylidene)isonicotinohydrazone and Investigation of Their Antibacterial and Antioxidant Properties

Farzana Khanm Camellia [a*], Md. Ashrafuzzaman [a], Md. Nazrul Islam [a], Laila Arjuman Banu [a] and Md. Kudrat-E-Zahan [a*]

[a] Department of Chemistry, University of Rajshahi, Rajshahi-6206, Bangladesh.

Authors' contributions

This work was carried out in collaboration among all authors. All authors read and approved the final manuscript.

Article Information

DOI: 10.9734/AJOCS/2022/v11i419130

Open Peer Review History:
This journal follows the Advanced Open Peer Review policy. Identity of the Reviewers, Editor(s) and additional Reviewers, peer review comments, different versions of the manuscript, comments of the editors, etc are available here: https://www.sdiarticle5.com/review-history/88253

Original Research Article

Received 02 April 2022
Accepted 10 June 2022
Published 14 June 2022

ABSTRACT

Cr^{3+}, Co^{2+}, Ni^{2+}, Cu^{2+} and Zn^{2+} ions complexes of the Schiff base ligand, N-(4-hydroxybenzylidene)isonicotinohydrazone (L1), were synthesized and characterized by analytical and physicochemical techniques including conductivity measurements, magnetic susceptibility measurements, IR Spectroscopy, UV-Visible Spectrophotometry and thermogravimetric analysis (TGA). IR data revealed the bidentate nature of the L1. IR, TGA, Magnetic moment measurements and UV-Vis spectra data confirmed the octahedral geometry for the Cr^{3+}, Co^{2+}, and Cu^{2+} ion complexes, square planar geometry for the Ni^{2+} complex and tetrahedral structure for the Zn^{2+} ion complex. The antibacterial activity of the metal complexes derived from the L1 ligand were tested against *P. aeruginosa* and *E. coli.* All produced complexes demonstrated strong antibacterial efficacy against *P. aeruginosa* when compared to standard Kanamycin-30, with the greatest for the Ni^{2+} complex. On the other hand, when compared to all compounds, the Zn^{2+} complex demonstrated strong antibacterial efficacy against E. coli. Furthermore, the synthesized metal complexes exhibited moderate antioxidant activity than the L1. The antioxidant activity was found to follow the following sequence: BHT > CuL1 > CrL1 > NiL1 > CoL1 > ZnL1 > L1.

**Corresponding author: E-mail: farzanakhanm2012@gmail.com, kudrat.chem@ru.ac.bd;*

Keywords: Schiff base; Transition metal compounds; Isoniazid; Kanamycin-30; Antioxidant.

1. INTRODUCTION

Compounds with the azomethine group (-C=N-) are referred to as Schiff bases; they are generated from the condensation reaction between primary amines and carbonyl compounds having aldehydes or ketones [1-2]. In the last decade, Schiff base ligands have gained more attention mainly by reason of their wide uses in the field of catalysis, biomimetic modeling as well as designing molecular magnet molecules and because of their antimicrobial and antifungal activity [3-4]. Another noteworthy feature is that they form stable complexes with the majority of transition metal ions, which has made them an important family of ligands in coordination chemistry [5-7] as well as inorganic chemistry [8]. Furthermore, they have various applications in biological, clinical, analytical, electrochemistry, medicinal, and industrial studies in addition to they are used as liquid crystals in the field of analytical, medicinal, and polymer chemistry [9-11]. Aside from that, Schiff bases and their complexes have biological actions that include antibiotic, antifungal, antibacterial, anti-inflammatory, anti-tumor, anti-oxidative, anti-HIV, and anti-cancer properties [12-15]. Isoniazid is a very effective medicine that is used as the first-line therapy for TB (tuberculosis). It is a suggested therapeutic material for Mycobacterium TB due to its high level of antibacterial activity. It forms metal chelate complexes with several physiologically important bivalent ions [16–19]. We disclosed here the synthesis and characterization of Schiff base, N-(4-hydroxybenzylidene) isonicotinohydrazone obtained from the condensation reaction of p-hydroxybenzaldehyde and isoniazid and its metal complexes of Cr^{3+}, Co^{2+}, Ni^{2+}, Cu^{2+}, and Zn^{2+}. Some bioactivity test findings, such as antibacterial and antioxidant properties for ligands and their metal complexes were also mentioned.

2. EXPERIMENTAL METHODS

All required chemicals with 99.9% purity were purchased from Merck and Loba chemicals. A METTLER PM 200 electronic balance was used to complete the weighing process. All produced metal complexes' melting or decomposition temperatures were measured using an electrothermal melting point equipment type o.AZ6512. The IR spectra of the produced compounds were acquired using a KBr disc on an FTIR-8400, SHIMADZU, Japan. The complexes' conductivities were measured in DMSO using a Horiba conductivity meter B173 with a set cell constant. The UV-Vis spectra of the ligand and its complexes were measured using a THERMOELECTRON NICOLET evolution 300 UV-Visible Spectrophotometers in DMSO solution (1×10^{-5} M). Sherwood Scientific Magnetic Susceptibility Balance was used in order to determine the values of all complexes' magnetic moments. The Perkin Elmer Simultaneous Thermal Analyzer, STA-8000, conducted the thermogravimetric analysis (TGA). Thin Layer Chromatography (TLC) was used to assess the ligand's purity and its metal complexes.

2.1 Synthesis of the Schiff base, N-(-4-hydroxybenzylidene)isonicotinohydrazone, (L1)

N-(4-hydroxybenzylidene)isonicotinohydrazone Schiff base Ligand, L1 was obtained (Scheme 1) by the conventional condensation reaction of p-hydroxybenzaldehyde with isoniazid (INH) in an equimolar ratio (i.e., 1:1). A methanolic solution of INH(1.37 g, 10.00 mmol) was taken in a round bottom flask, and then a methanolic solution of 4-hydroxybenzaldehyde (1.22 g, 10.00 mmol) was added to it with continuous stirring. As a catalyst, little amount of glacial acetic acid (2-3 drops) was added dropwise to this mixture. The resultant mixture was allowed to reflux for about 4 hours. TLC monitored the purity of the obtained product throughout the whole reaction. A light-yellow precipitate of the ligand was produced, which was then filtered and washed several times with cold CH_3OH solution before being dried in a desiccator over anhydrous $CaCl_2$.

2.2 General Procedure for Synthesis of Metal Complexes

15 mL warm ethanolic solutions (1 mmol) of nitrate salts of metal (Cr^{3+}, Co^{2+}, Ni^{2+}, Cu^{2+} and Zn^{2+}) were slowly added to the warm ethanolic solution (15 mL) of Schiff base ligand L1 (2 mmol) in a reflux set. The resulting mixture was refluxed for about 4 h. After cooling, the obtained precipitates were filtered and washed with cold C_2H_5OH solution and dried under vacuum on anhydrous $CaCl_2$. A reference complex, having composition $[Cu(L1)_2(H_2O)_2]Cl_2$ symbolized as CuCL1 has also prepared according to the above procedure for comparative antibacterial study.

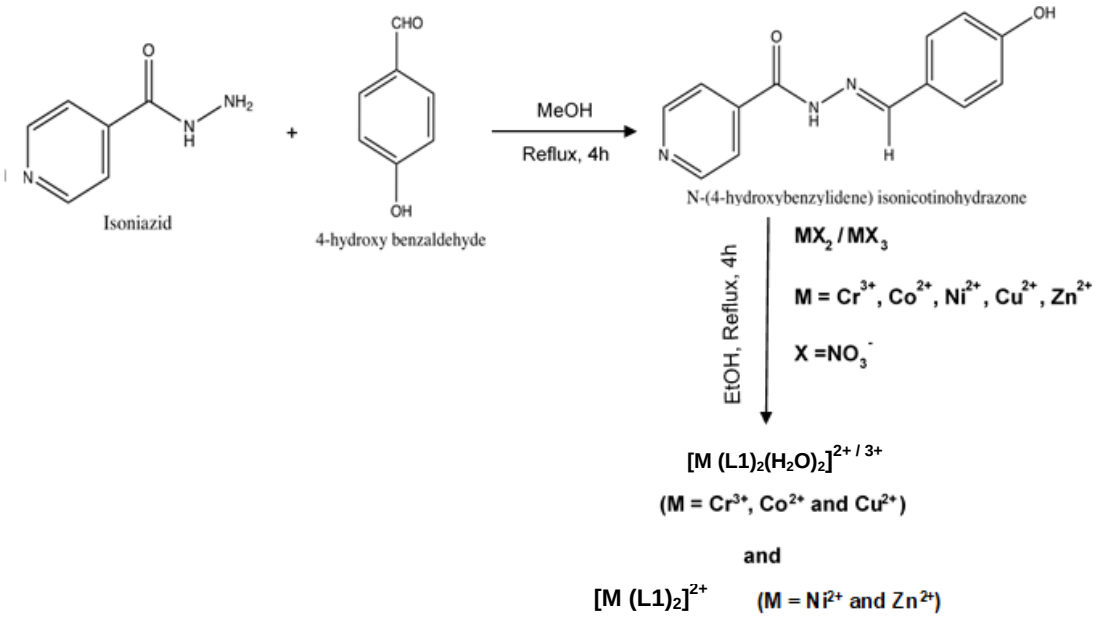

Scheme 1. Synthesis of the Schiff base ligand, L1 and its metal complexes

2.3 Antibacterial Studies

Antimicrobial activity of the ligand and its complexes were performed against *P. aeruginosa* and *E. coli* in DMSO by disc diffusion approach [20-21]. All pathogenic bacteria under this study were collected from the Department of Pharmacy, University of Rajshahi, Rajshahi-6205, Bangladesh.

2.4 Antioxidant Studies

The DPPH free radical scavenging technique was used to calculate antioxidant activity. The inhibition percentage, which was associated with the compounds' radical scavenging activity, was calculated by using the following formula [22]:

DPPH Scavenging Activity (%) = $(A_o\text{-}A_{sample})/A_o \times 100$

Where A_o is the absorbance of blank and A_{sample} is the absorbance of the tested sample.

Calculation of IC_{50} values: In order to get the IC_{50} value, a linear regression was performed between the percentage inhibition and log concentration. Higher antioxidant activity is indicated by a lower IC_{50} value [23].

3. RESULTS AND DISCUSSION

All of the produced complexes were insoluble in polar solvents, although they were soluble in DMSO and DMF. At room temperature, the molar conductance values of all generated complexes (10^{-3} M) were tested in DMSO solution. The physical properties of the L1 and its metal complexes have shown in Table 1. The conductivity of the Cr^{3+} complex was determined to be 160 $ohm^{-1}cm^2mol^{-1}$, implying a 1:3 electrolyte, whereas other complexes were 1: 2 electrolytes [24-25]. The magnetic moments for Cr^{3+}, Co^{2+}, Ni^{2+}, Cu^{2+} and Zn^{2+} complexes were 3.73 BM, 4.81 BM, 0.43 BM, 1.78 BM, and 0.62 BM, respectively. The magnetic moment's value of the Cr^{3+} complex indicated the octahedral geometry [26] having three unpaired electrons, slightly less than the spin-only value (3.88 BM). Complexes having three unpaired electrons might be tetrahedral or octahedral geometry. Magnetic moments for the high-spin octahedral Co^{2+} complexes range from 4.7 to 5.2 B.M. The Co^{2+} has a ground state of $^4T_{1g}$ in an octahedral complex, which contributes a large orbital moment to magnetic moments. Therefore, the observed magnetic moment's value of the Co^{2+} complex supported its octahedral structure rather than tetrahedral [27]. For tetrahedral Ni^{2+} complex, the magnetic moment value should be in the range of 3.4 to 4.2 BM. The possible reasons for the increasing magnetic moment compared to that of spin only value has already been disclosed by Nyholm et al. [27]. However, the magnetic moment of the Ni^{2+} complex was 0.43 BM, suggesting its diamagnetic nature and square planar geometry [28]. For the Cu^{2+}

complex, the magnetic moment indicates its paramagnetic nature, and the mentioned value corresponds to octahedral geometry [29]. Similarly, the magnetic moment of the Zn^{2+} complex corresponds to its diamagnetic nature as well as its tetrahedral environment [30].

3.1 IR Spectral Studies

The IR spectra of the ligand, L1 has presented in the Fig. 1. The IR spectra of the ligand revealed a strong band at 1658 cm^{-1} owing to the ν (C=O) of the amide group. In all complexes (Figs. 2-6), this intense band has moved to lower frequencies demonstrating coordination via the oxygen atom of carbonyl (C=O) group. The azomethine group ν (C=N) band positioned at 1598 cm^{-1} has shifted to lower frequencies in all complexes, showing that the azomethine nitrogen (N) is engaged in coordination [31]. Due to the combined mode of ν(O-H) and N-H stretching vibrations, a broad, strong band developed in the range of 3467-3434 cm^{-1}. The appearance of a new band at 1025 cm^{-1} owing to δH_2O supports the existence of coordinated water in complexes [32] except NiL1 and ZnL1 complexes. The existence of coordinated water was further confirmed by the TGA data summarized in the Table 4. Along with this, the complexes' IR spectra revealed additional non-ligand bands in the ranges between 588-560 and 494-464 cm^{-1}, which were designated as M-O (metal to oxygen) and M-N stretching vibrations, respectively [33-34]. Consequently, it may be concluded that the ligand (L1) interacts with the metal ions via the nitrogen (N) and oxygen (O) atoms in the azomethine and carbonyl groups of its structure. However, all observations with assignments have given in the Table 2.

Table 1. Physical properties of the L1 and its metal complexes

Ligand/Complexes (Symbol)	Appearance and body color	M.W	% Yield	M.P/Deo (C)	Molar Conductivity (ohm cm^2 mol^{-1})	μ eff (B.M)
$C_{13}H_{11}N_3O_2$ (L1)	Light yellow powder	241.2	75%	185	NA	NA
$[Cr(L1)_2(H_2O)_2](NO_3)_3$ (CrL1)	Dark brown powder	756.4	71%	>300	160	3.73
$[Co(L1)_2(H_2O)_2](NO_3)_2$ (CoL1)	Brown powder	701.4	69%	>300	121	4.81
$[Ni(L1)_2](NO_3)_2$ (NiL1)	Crimsonpowder	665.1	72%	>300	115	0.43
$[Cu(L1)_2(H_2O)_2](NO_3)_2$ (CuL1)	Green powder	706.4	78%	>300	125	1.78
$[Zn(L1)_2](NO_3)_2$ (ZnL1)	White powder	671.8	71%	>300	119	Dia

Table 2. Key Infrared bands (cm^{-1}) of ligand L1 and its metal complexes

Ligand/ Complexes	$\nu_{(OH)}$ +$\nu_{(NH)}$	$\nu_{(C=O)}$	$\nu_{(C=N)}$	$\nu_{(M-O)}$	$\nu_{(M-N)}$
L1	3232	1658	1598	--	--
CrL1	3435	1637	1585	588	492
CoL1	3436	1600	1571	560	464
NiL1	3434	1649	1597	578	494
CuL1	3436	1614	1591	573	484
ZnL1	3467	1621	1553	580	484

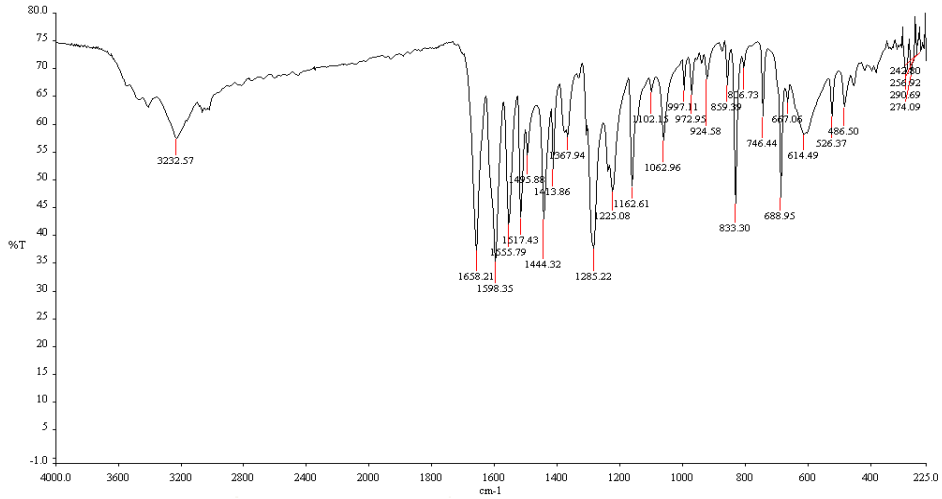

Fig. 1. IR spectrum of L1

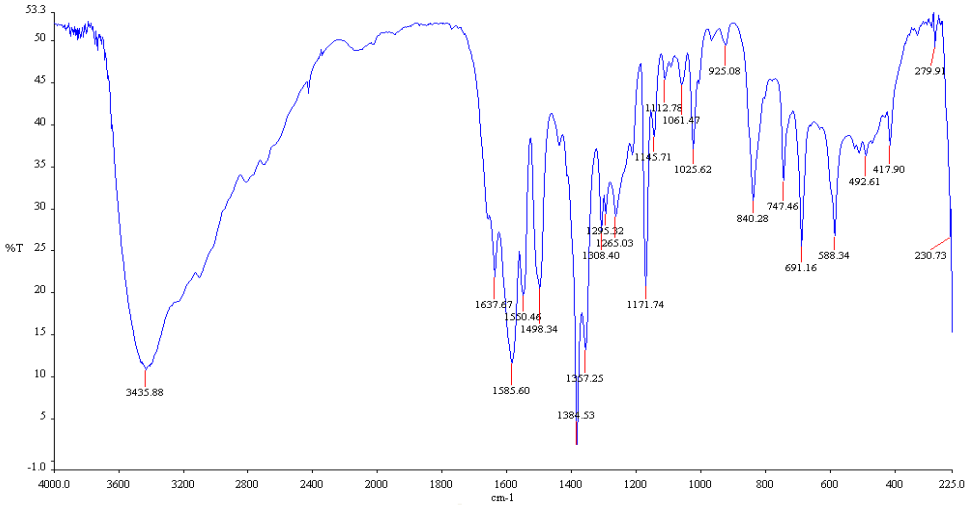

Fig. 2. IR spectrum of CrL1

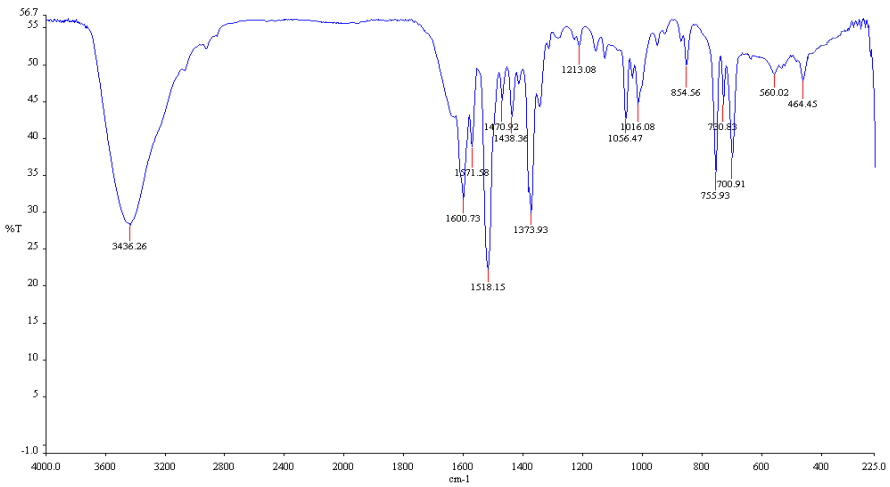

Fig. 3. IR spectrum of CoL1

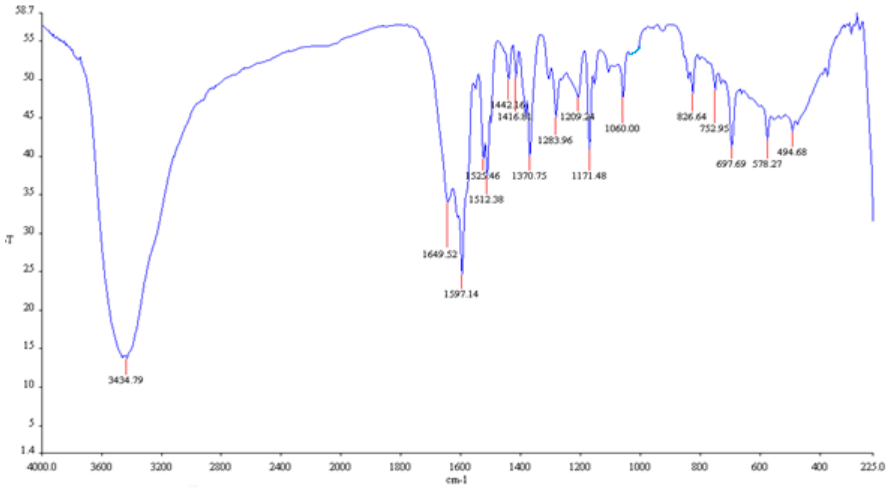

Fig. 4. IR spectrum of NiL1

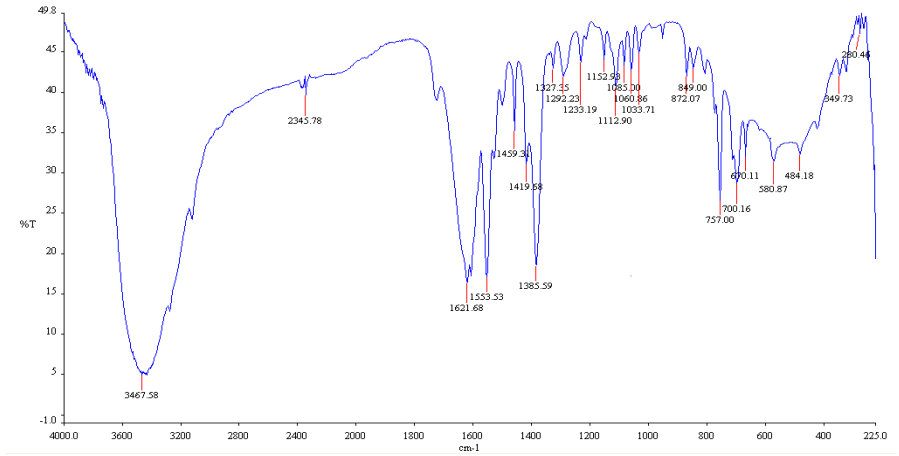

Fig. 5. IR spectrum of CuL1

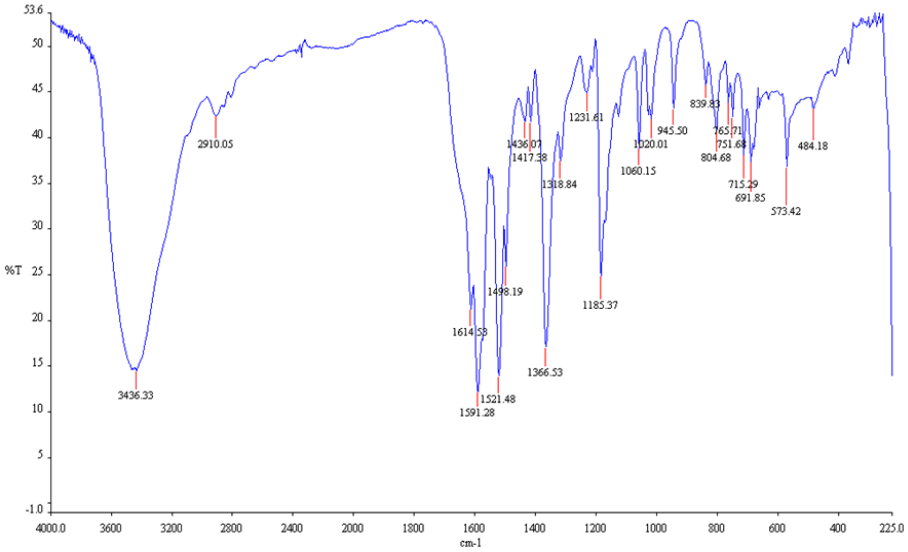

Fig. 6. IR spectrum of ZnL1

3.2 Electronic Spectra

L1 showed two distinct bands at 271 and 324 nm, which were for π-π* and n-π* transitions, respectively (Fig. 7). For the CrL1 complex, three bands were identified at 282, 351, and 440 nm. The band at 282 nm owing to the π-π* transition is marginally altered by chelation in comparison to the free ligand. In contrast, the band at 351 nm, which corresponds to azomethine, broadened and shifted to a longer wavelength, showing the involvement of ligand to metal through the azomethine molecule. However, the band positioned at 440 nm is due to the d-d transition [26]. There were four bands at 271, 336, 380, and 460 nm for the CoL1 complex. The absorption band centered at 380 nm may be related to the ligand to metal charge transfer (LMCT) transition. The band at 460 nm corresponds to the $^4T_{1g}$ (F)→ $^4T_{1g}$ (P) transition, which is indicative of octahedral geometry [35]. The NiL1 complex, like the other complexes, exhibited the transitions stated above. In the case of square planar Ni^{2+} complex, there should have a d-d transition above 500 nm, but this band was not observed in our research work. The CuL1 complex also showed three bands at 270, 360 and 532 nm, respectively. The band centered at 532 nm, is a d-d absorption band, which is attributed to $^2E_g \rightarrow {}^2T_{2g}$ transition suggesting the octahedral geometry of this complex [36]. The ZnL1 complex also showed three bands positioned at 270, 339 and 354 nm. The ZnL1 complex with a d^{10} electronic configuration displayed a band at 354 nm due to the LMCT transition, which corresponds well with the tetrahedral geometry [37]. All observations have presented in the tabulated form in Table 3.

3.3 Thermogravimetric Analysis (TGA)

TGA studies were carried out on complexes in a nitrogen (N_2) gas atmosphere in the temperature range of 25-800 ^oC. The thermogram of complexes exhibits multi-stage weight loss [Figs. 8-10]. For the CrL1 complex, the first step occurred at around 250°C due to the elimination of two coordinated H_2O molecules (calcd. 4.76%, found 4.74%) [38]. In the temperature range of 250-380 ^oC, 35.70% weight loss was found (calcd. 35.72%), which was due to the removal of $2C_6H_5N_3O$ (part of the ligand). Third weight loss (calcd. 49.46%, found 49.31 %) due to the removal of another part of ligand ($2C_7H_6O$) along with some gases (i.e., NO_2 and O_2) was observed in the temperature range of 380-680 ^oC. Above 680 ^oC, no weight loss was observed in the TGA curve of the CrL1 complex. This may be due to the formation of metallic oxide (Cr_2O_3) [39]. For CoL1 complex, first weight loss (calcd. 5.14 %, found 5.13 %) was observed around 200 ^oC suggesting the removal of two molecules of coordinating water. The second step of decomposition was observed with a mass loss of 83.84 % (calcd. 84.18 %) within the range of 200-650 ^oC of indicating the dissociation of ligands together with some gases leaving CoO as residue. In the case of the CuL1 complex, the

Table 3. Key UV bands (nm) of ligand L1 and its metal complexes

Ligand/ Complexes	Band Positions (nm)	Assignment	Geometry
L1	271	π → π*,	
	324	n → π*	
CrL1	282	π → π*,	Octahedral
	351	n → π*	
	440	**$^4A_{2g}$ (F) → $^4T_{1g}$ (P)**	
CoL1	271	π → π*,	Octahedral
	336	n → π*	
	380	CT	
	460	**$^4T_{1g}$ (F) → $^4T_{1g}$ (P)**	
NiL1	274	π → π*,	Square planar
	341	n → π*	
CuL1	270	π → π*,	Octahedral
	360	n → π*	
	532	**$^2E_g \rightarrow {}^2T_{2g}$**	
ZnL1	270	π → π*,	Tetrahedral
	339	n → π*	
	354	CT	

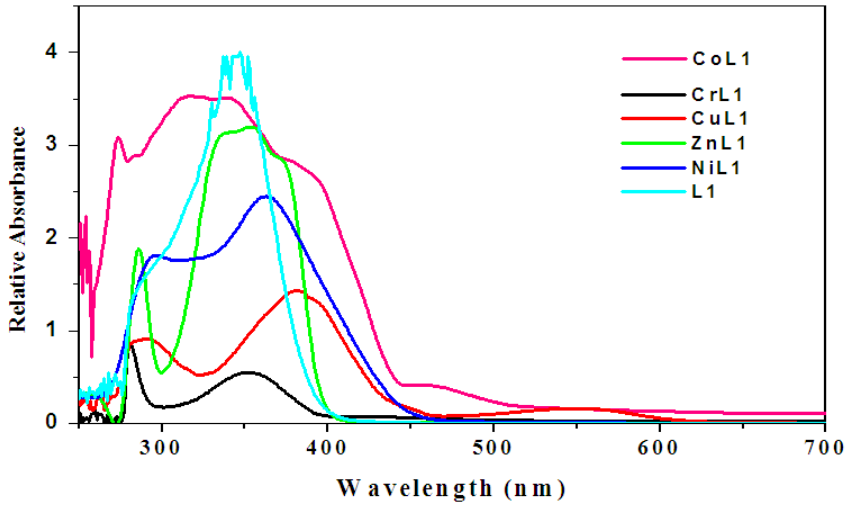

Fig. 7. UV-Vis spectra of L1 and its metal complexes

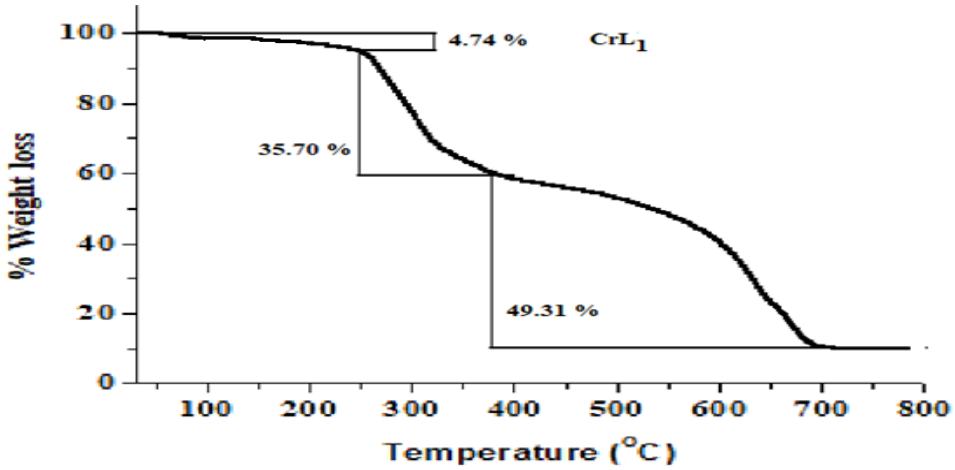

Fig. 8. TGA curve of CrL1 complex

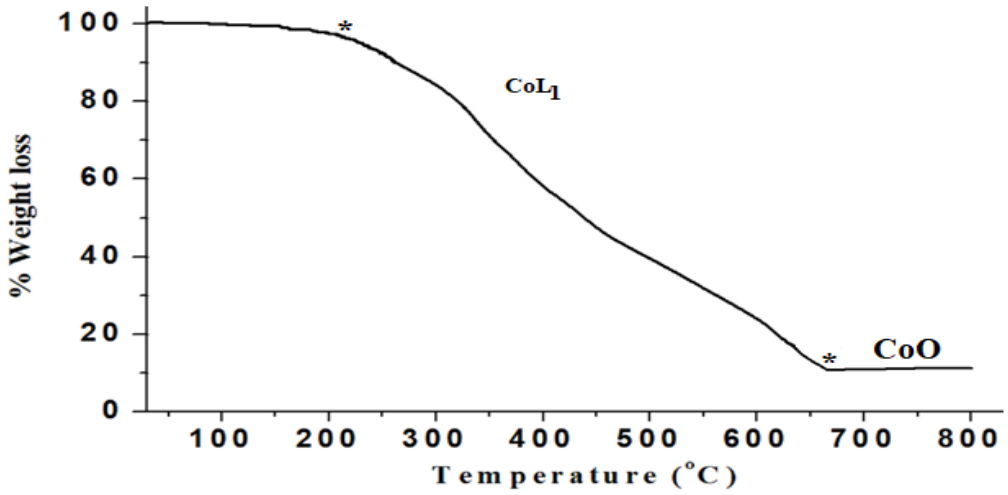

Fig. 9. The TGA curve of CoL1 complex

TGA curve showed three steps of decomposition up to 680 °C. The first stage (like other complexes) at around 235 °C with a weight loss of 5.13 % (calcd. 5.10 %) confirmed the presence of two coordinated water molecules. The second step with a mass loss of 30.08 % (calcd. 30.05) at 235-375 °C, corresponds to the loss of $2C_6H_4NO$ (part of ligand). The penultimate step in the range of 375-680 °C, having a mass loss of 53.75 % (calcd. 53.56 %) supports the elimination of the residual ligand ($2C_7H_7N_2O$) as well as some gases. The final residue with a constant weight represents CuO [40].

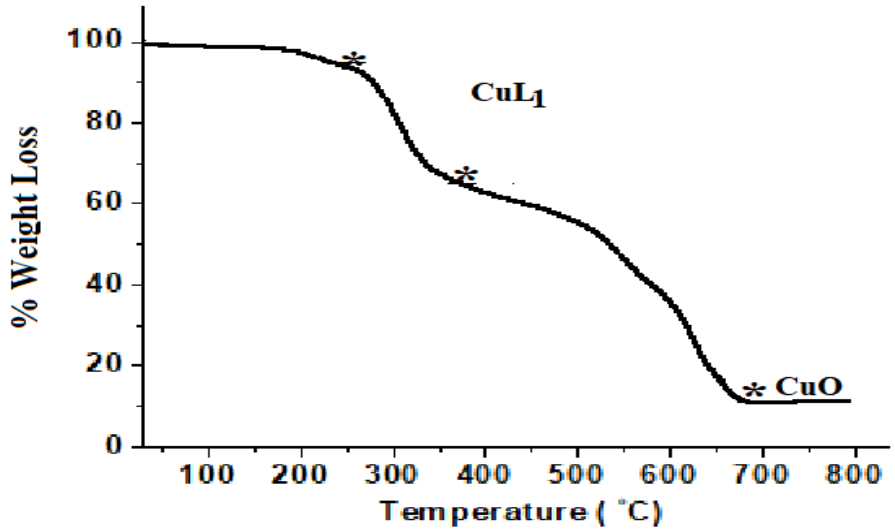

Fig. 10. The TGA curve of CuL1 complex

Table 4. Thermoanalytical data of CrL1, CoL1 and CuL1 complexes

Complex	Temperature Range (°C)	Weight loss (%)		Assignments
		Found	Calculated	
CrL1	30 – 250	4.74	4.76	Loss of two coordinated H_2O molecules
	250-380	35.70	35.72	$2C_6H_5N_3O$
	380-680	49.31	49.46	$2C_7H_6O + 3NO_2 + 0.75\ O_2$
	> 680	10.25	10.05	$0.5\ Cr_2O_3$
CoL1	30 – 200	5.13	5.14	Loss of two coordinated H_2O molecules
	200-650	83.84	84.18	$2\ L1 + 2NO_2 + 0.5\ O_2$
	> 650	11.03	10.68	CoO
CuL1	30 – 235	5.13	5.10	Loss of two coordinated H_2O molecules
	235-375	30.08	30.05	$2C_6H_4NO$
	375-680	53.75	53.56	$2C_7H_7N_2O + 2NO_2 + 0.5\ O_2$
	> 680	11.04	11.26	CuO

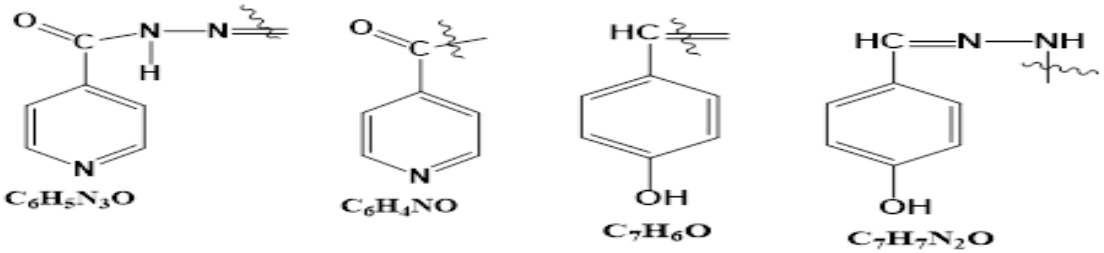

Proposed Structure: On the basis of above characterizations, the following structures can be proposed for the obtained metal complexes.

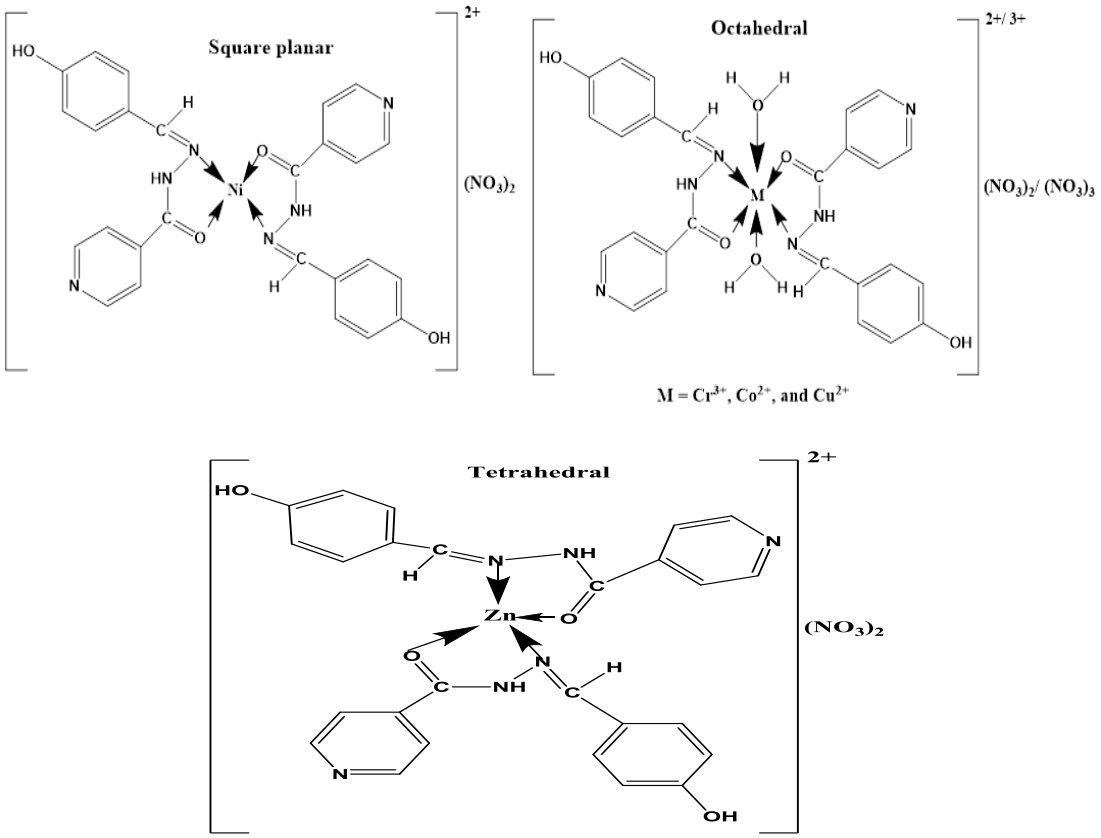

Table 5. Antibacterial activities of ligand L1 and its metal complexes

Diameter of Zone of Inhibition (mm) of tested compounds (100µg/disc)		
Compounds	**Gram Negative**	
	Escherichia coli	***Pseudomonas* aeruginosa**
Kanamycin (30 µg/disc)	30	15
Ligand (L1)	07	10
CrL1	20	21
CoL1	21	18
NiL1	20	25
CuL1	23	23
CuCL1 (Ref.)	15	17
ZnL1	25	15

3.4 Antibacterial Activity

The antibacterial activity of Schiff base ligands and its metal complexes against *Escherichia coli* and *Pseudomonas aeruginosa* was studied at a concentration of 100 µg/ 10 µL in DMSO. The diameter of the inhibitory zone was measured in millimeters, and the results of their antibacterial activity have presented in Table 5. The metal complexes showed more antibacterial activity than free ligand against two pathogenic bacteria. Among all synthesized complexes, the Ni^{2+} complex showed good antibacterial activity against *Pseudomonas aeruginosa* and the following trend is observed: NiL1> CuL1> CrL1> CoL1> CuCL1(Ref.) > ZnL1 = Kanamycin-30> L (Fig. 11). On the other hand, the Zn^{2+} complex showed good activity against E. coli when compared with all synthesized compounds. In this case the order of the antibacterial activity

follows the following trend: Kanamycin-30 > ZnL1> CuL1> CoL1 > CrL1= NiL1 > CuCL1(Ref.) > L1. Some factors such as the lipophilic nature of metal complexes, solubility, coordinating sites, complex geometry, steric hindrance, concentration, and hydrophobicity have a significant impact on antibacterial potency [41-43]. However, the increased antibacterial activity of metal complexes compared to the free ligand can be well understood by Overtone's idea and Tweedy's chelation hypothesis [41].

3.5 Antioxidant Activity

The antioxidant properties of L1 and its metal ion complexes were evaluated using the free radical molecule 1, 1-Diphenyl-1-picryl hydrazyl (DPPH). Table 6 displays the percentage of DPPH radical scavenging activity of L1, metal complexes, as well as BHT (butylated hydroxytoluene) as a reference. According to the findings, all of the metal complexes showed moderate DPPH radical scavenging activity (Fig. 12). The order can be given as BHT> CuL1> CrL1> NiL1> CoL1> ZnL1 >L1. The redox characteristics and coordination environment of the Schiff base metal complexes may explain the variance in antioxidant activity. Several variables impact the redox characteristics of metal complexes, including chelate ring size, chelate ring unsaturation and axial ligation. [42,43]. Since the Zn^{2+} ion is not a transition metal and therefore cannot participate in electron-transfer processes, its activity is reduced [44]. On the other hand, the Cu^{2+} complex has higher antioxidant activity than other synthesized complexes may be due to its reducing ability and proton donation characteristic, which allows Cu^{2+} to serve as a superoxide scavenging center [44]. As a consequence, the findings of this research suggest that the CuL1 complex might be used to treat pathological disorders caused by oxidative stress. The IC_{50} value of all stated compounds in combination with standard BHT has been calculated and shown in Fig. 13.

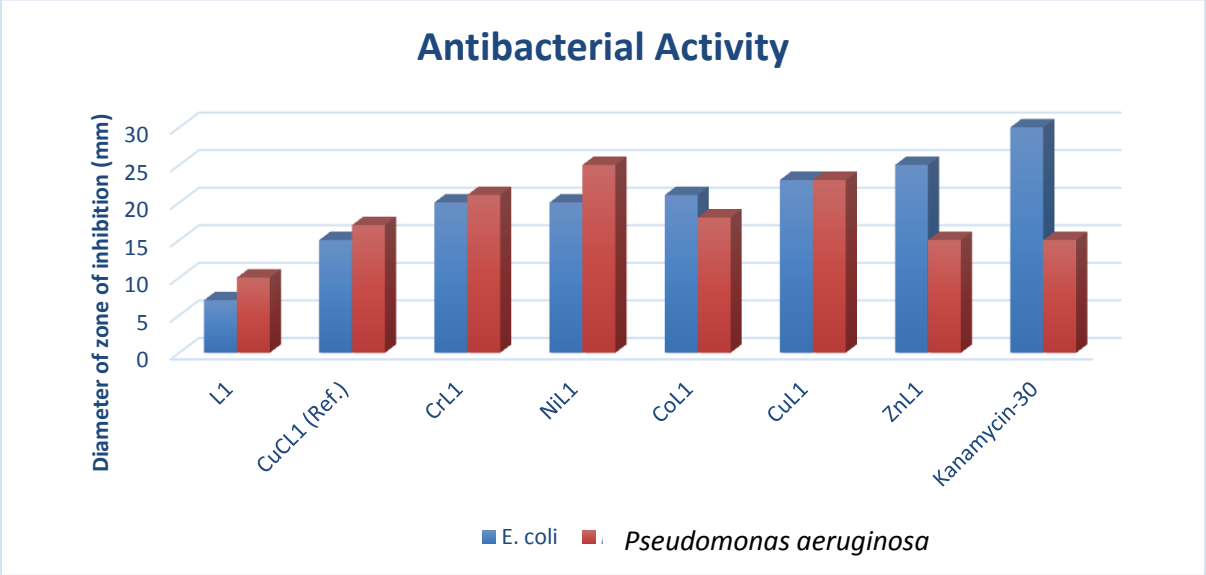

Fig. 11. Graphical representation of antibacterial activity of ligand L1 and its metal complexes against *Escherichia coli* and *Pseudomonas aeruginosa* with standard Kanamycin-30 and ref

Table 6. % of Scavenging activity of BHT, ligand L1, and its metal complexes

Conc. (µg/mL)	% BHT	% L1	% CrL1	% CoL1	% NiL1	% CuL1	% ZnL1
20	12.41	1.38	5.34	3.75	2.69	10.7	2.34
40	27	2.87	15.25	10.97	3.54	24.13	5.61
60	36.98	4.11	17.83	12.88	5.09	29.56	6.72
80	41.2	6.02	19.62	14.65	7.50	31.77	8.24
100	45.78	6.99	22	15.27	9.34	32.28	8.91

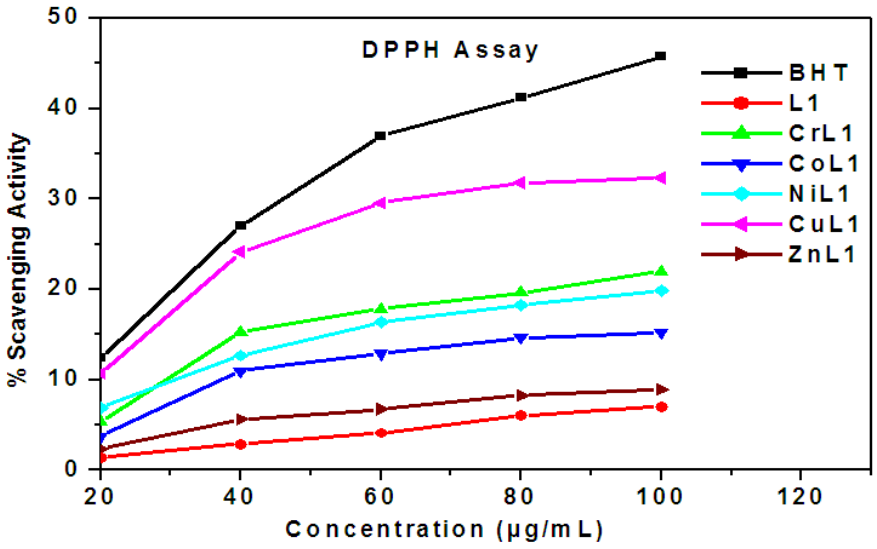

Fig. 12. DPPH radical scavenging activity of the L1 and its metal ions complexes at different concentrations (20, 40, 60, 80, and 100 µg/mL) with standard BHT

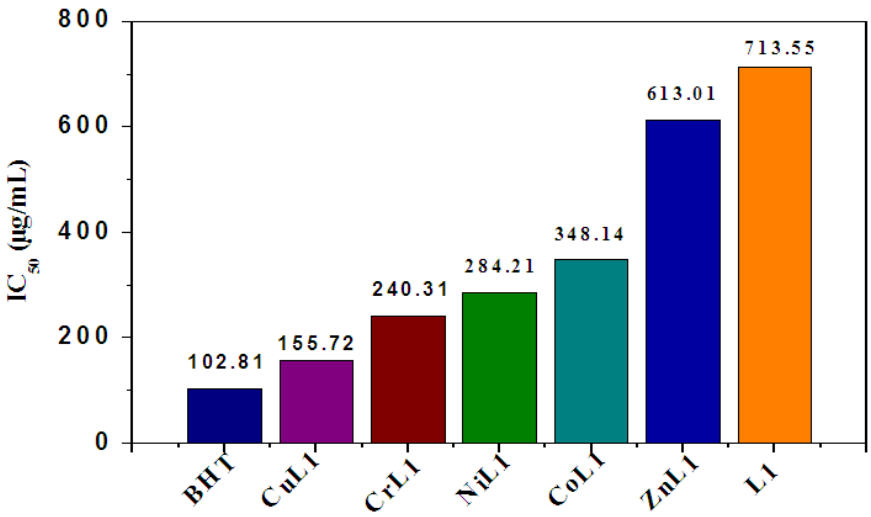

Fig. 13. IC_{50} IC50 value of the metal complexes of ligand L1 at various concentrations (20, 40, 60, 80, and 100 µg/mL) with standard BHT

4. CONCLUSION

Condensation of 4-hydroxybenzaldehyde with isoniazid results in the formation of a novel bidentate Schiff base ligand. When compared to the Kanamycin-30, all produced complexes were determined to be more active against *P. aeruginosa*. The antibacterial activity of the CuL1 complex against two different pathogenic bacteria is particularly remarkable. The antioxidant activity of the CuL1 complex was the greatest among all the complexes when compared to that of BHT. Further research is needed before CuL1 can be used as a possible medication to treat oxidative stress.

ACKNOWLEDGMENTS

The authors are thankful to the Chairman, Department of Chemistry, University of Rajshahi, Bangladesh for the laboratory Facilities.

COMPETING INTERESTS

Authors have declared that they have no known competing financial interests or non-financial

interests or personal relationships that could have appeared to influence the work reported in this paper.

REFERENCES

1. Thorat BR, Kamat P, Khandekar D, Lele S, Mustapha M, Sawant S, Jadhav R, Kolekar S, Yamgar R, Atram RG. Synthesis and Fluorescence study of Novel Schiff Bases of Isoniazide. J. Chem. Pharm. Res. 2011;3(6):1109-1117.
2. Naganagowda G, Meijboom R, Petsom A. Synthesis and Antimicrobial Activity of New Schiff Base Compounds Containing 2-Hydroxy-4-pentadecylbenzaldehyde Moiety. Adv. Chem. 2014;1-9.
3. Kotkar SN, Juneja HD. Synthesis, Characterization, and Antimicrobial Studies of N, O Donor Schiff Base Polymeric Complexes. J. Chem. 2013;1-5. DOI: doi.org/10.1155/2013/479343
4. Ahmed RM, Yousif EI, Al-Jeboori MJ. Co(II) and Cd(II) Complexes Derived from Heterocyclic Schiff-Bases: Synthesis, Structural Characterisation, and Biological Activity. The Sci. World J. 2013; 1-7. DOI: org/10.1155/2013/754868
5. Gupta B, Fahmi N. Co(II) and Ni(II) Complexes with Schiff Base Ligands: Synthesis, Characterization, and Biological Activity. R. J. Gen. Chem. 2016;86(5): 1182–1190.
6. Patange AN, Yadav UM, Desai PA, Singare PU. Synthesis of some Novel Halogenated Platinum (II) Complexes of Active Schiff's Base Ligand Derived from 5-Bromo Isatin and Evaluation of their Antibacterial Activity. W. Sci. News. 2015;10:32-43.
7. Rosenberg B, Vancamp L, Krigas T. Inhibition of Cell Division in Escherichia coli by Electrolysis Products from a Platinum Electrode. Nature. 1965;205:698-699.
8. Ababei LV, Kriza A, Andronescu C, Musuc AM. Synthesis and characterization of new complexes of some divalent transition metals with 2-acetyl-pyridyl-isonicotinoylhydrazone. J. Therm. Anal. Calorim. 2012;107:573–584.
9. Radfard R, Abedi A. Synthesis and Characterization of New Schiff Bases of Ethylenediamine and Benzaldehyde Derivatives, Along with Their Iron Complexes. J. Appli. Chemi. Res. 2015; 9(2):59-65.
10. Obasuyi EI, Iyekowa O. Synthesis, Characterization and Antimicrobial of Schfiff Base from 5-Bromo – Salicylaldehyde and P-Toluidine. J. Appl. Sci. Environ. Management. 2018;22(11): 1733–1736.
11. Rao VK, Reddy SS, Krishna BS, Naidu KRM, Raju CN, Ghosh SK. Synthesis of Schiff bases in aqueous medium: a green alternative approach with effective mass yield and high reaction rates. Gr. Chem. Lett. Review. 2010; 3(3):217-223.
12. Saadeh HA, Abu Shaireh EA, Mosleh IM, Al-Bakri AG, Mubarak MS. Synthesis, characterization and biological activity of Schiff bases derived from metronidazole. Med. Chem. Res. 2012; 21:2969–2974.
13. Dhayabaran VV, Prakash TD, Renganathan R, Friehs E, Bahnemann DW. Novel Bioactive Co(II), Cu(II), Ni(II) and Zn(II) Complexes with Schiff Base Ligand Derived from Histidine and 1,3-Indandione: Synthesis, Structural Elucidation, Biological Investigation and Docking Analysis. J. Fluoresc; 2016. DOI 10.1007/s10895-016-1941-x
14. Abdel-Rahman LH, El-Khatib RM, Nassr LAE, Abu-Dief AM. DNA binding ability mode, spectroscopic studies, hydrophobicity, and in vitro antibacterial evaluation of some new Fe(II) complexes bearing ONO donors amino acid Schiff bases. Arb. J. Chem; 2013. DOI: doi.org/10.1016/j.arabjc.2013.07.010
15. Prashanthi Y, Kiranmai K, Ira. S. Kumar, Chityala VK, Shivaraj. Spectroscopic Characterization and Biological Activity of Mixed Ligand Complexes of Ni(II) with 1,10 Phenanthroline and Heterocyclic Schiff Bases. Bioinorg. Chem. Appli. 2012;1-9. DOI: 101155/2012/948534
16. Anoop KP, Abhishek B, Vikas B, Apoorva D. Structural, Electronic, and Vibrational Properties of Isoniazid and Its Derivative N-Cyclopentylidenepyridine-4-carbohydrazide: A Quantum Chemical Study, J. Theoret. Chem. 2014;1-15.
17. Garner RN, Pierce CG, Reed CR, Brennessel WW. Photoinitiated Treatment of Mycobacterium using Ru (II) Isoniazid Complexes, Inorganica. Chimica. Acta. 2017;461:261-266.
18. Zubatyuk RI, Kucherenko LI, Mazur IA, Khromyleva OV, Shishkin OV. A theoretical structural study of isoniazid complexes with thiotriazoline, Chem. Hetero. Comp. 2014;50(3):476-482.

19. Guilian L, Jingrui Z, Yi J, Li-li Z, Haican L, Machao LL, Xiuqin Z, Kanglin W. Cross-resistance of isoniazid, para-aminosalicylic acid and pasiniazid against isoniazid-resistant Mycobacterium tuberculosis isolates in China, J. Glob. Antimicro. Resist. 2020;20:275–281.
20. Hossain MS, Islam MA, Zakaria CM, Haque MM, Mannan MA, Zahan MK. Synthesis, spectral and thermal characterization with antimicrobial studies on Mn(II), Fe(II), Co(II) and Sn(II) complexes of tridentate N,O coordinating novel Schiff base ligand, J. Chem. Bio. Phy. Sci. 2016;6(1):041-045.
21. Shiraj-U-Ddula M, Islam MA, Akhter S, Islam MK, Zahan MK. Synthesis, Characterization and Antimicrobial Activity of Cd(II), Ni(II), Co(II) and Zr(IV) Metal Complexes of Schiff Base Ligand Derived from Diethylenetriamine and Isatin, Asian J. Res. Chem. 2014;7(7):45-49.
22. Bingöl M, Turan N. Schiff base and metal(II) complexes containing thiophene-3-carboxylate: Synthesis, characterization and antioxidant activities, J. Molecul. Struct. 2020;1205:01-07.
DOI: org/101016/j.molstruc.2019.127542.
23. Shekhar TC, Anju G. Antioxidant Activity by DPPH Radical Scavenging Method of Ageratum conyzoides Linn. Leaves, Amer. J. Ethnomed. 20141(4):244—249.
24. Ali I, Wani AW, Kishwar S. Empirical Formulae to Molecular Structures of Metal Complexes by Molar Conductance, Synthesis and Reactivity in Inorganic, Metal-Org. Nano-Met. Chem. 2013;43(9):1162-1170.
25. Mariana LD, Angela K, Nicoale S, Adin MM. Transition metal M(II) complexes with isonicotinic acid 2-(9-anthrylmethylene)-hydrazide, J. Serb. Chem. Soc. 2010; 75:1515-1520.
26. Santhi S, Namboori CGR. Synthesis, Characterization and Spectral Studies of Fe(III) and Cr(III) Schiff base Complexes with Acetoacetanilid- epropylenediamine, Oriet. J. Chem. 2011;27(3):1203-1208.
27. Figgis BN, Nyholm RS. 60. Magnetochemistry. Part I. Introduction and apparatus. J. Chem. Soc. 1959;12:331-338.
DOI:101039/JR9590000331
28. Chandra S, Gupta LK, Jain D. Spectroscopic studies on Mn(II), Co(II), Ni(II), and Cu(II) complexes with N-donor tetradentate (N4) macrocyclic ligand derived from ethylcinnamate moiety, Spectrochim. acta. Part A, Mole. Biomol. Spect. 2004;60(10):2411-2417.
29. Liu H, Wang H, Gao F, Niu D, Lu Z. Self-assembly of copper(II) complexes with substituted aroylhydrazones and monodentate N-heterocycles: synthesis, structure and properties, J. Coord. Chem. 2007;60(24):2671-2678.
30. Afsan F, Dalia SA, Hossain S, Sarkar S, Zahan KE. Synthesis, Spectral and Thermal Characterization of Selected Metal Complexes Containing Schiff Base Ligands with Antimicrobial Activities, Asian J. Chem. Sci. 2018;4(3):1-19.
31. Alarabi HI, Suayed WA. Microwave assisted synthesis, characterization, and antimicrobial studies of transition metal complexes of schiff base ligand derived from isoniazid with 2-hydroxyna-phthaldehyde, J. Chemi. Pharma. Res. 2014;6(1):595-602.
32. Tripathy SK, Panda A, Das PK, Behera NK, Panda AK. Synthesis, characterization and antimicrobial activities of homo- and bimetallic trinuclear complexes of a 30-membered macrocyclic ligand, J. Indian Chem. Soc. 2014;91(7): 1237-1245.
33. Burns GR. Metal complexes of thiocarbohydrazide, Inorg. Chem. 1968;7: 272.
34. Khalil MMH, Ismail EH, Mohamed GG, Zayed EM, Badr A. Synthesis and characterization of a novel schiff base metal complexes and their application in determination of iron in different types of natural water, Open J. Inorg. Chem. 2012;2:13-21.
35. Krishna CH, Mahapatra CM, Dash KC. 4-, 5- and 6-coordinate complexes of copper(II) with substituted imidazoles, J. Inorg. Nucl. Chem. 1977;39:1253-1258.
36. Raman N, Ravichandran S, Thangaraja C. Copper(II), cobalt(II), nickel(II) and zinc(II) complexes of Schiff base derived from benzil-2,4-dinitropheny- lhydrazone with aniline, J. Chem. Sci. 2004;116 (4):215–219.
37. Kismat AE, Saddam HM, Nur ABM, Zahid AASM, Ranjan KM, Mannan MA, Zakaria CM, Zahan MKE. Synthesis, Spectral and Thermal Characterization on Bioactive Complexes of Mg(II), Zn(II), Sn(II) VO(II) and Bi(III) ions Containing Schiff Base Ligand. J. Chem. Bio. Phy. Sci. 2019; 9(4):201-218.

38. Bottei RS, Quane D. Preparation and thermal stability of some divalent metal chelate polymers of β-hydronaphthazarin, J. Inorg. Nucl. Chem., 1964;26:1919-1925.
39. Prasad KS, Kumar LS, Shekar SC, Prasad M, Revanasiddappa HD. Oxovanadium Complexes with Bidentate N, O Ligands: Synthesis, Characterization, DNA Binding, Nuclease Activity and Antimicrobial Studies, Chem. Scien. J. 2011;CSJ-12
40. Al–Bayati S, Rasheed A, Zuhair E, Abid K, Khamis W. Synthesis and Spectroscopic Studies of New Alkoxy Schiff Base Complexes Based on Coumarin Moiety, Amer. J. Chem. 2018;8(1):1-7.
41. Patel MN, Pansuriya PB, Parmar PA, Gandhi DS. Synthesis, characterization and thermal and biocidal aspects of drug-based metal complexes, Pharma. Chem. J. 2008;42(12):687-692.
42. Kadtala V, Nirmala G, Sreenu D, Kumar K, Krishnan R, Shivaraj. Crystal structure, DNA interactions, antioxidant and antitumor activity of thermally stable Cu(II), Ni(II) and Co(II) complexes of an N,O donor Schiff base ligand, Poly. 2019; 171:86–97.
43. Sumalatha V, Aveli R, Narendrula V, Nirmala G, Sreenu D, Shivaraj. Synthesis, characterization, DNA binding propensity, neuclease efficacy, antioxidant and antimicrobial activities of Cu(II), Co(II) and Ni(II) complexes derived from 4-(trifluromethoxy) aniline Schiff bases. Chem. Data Collect. 2019;20:1-12.
44. Saif M, El-Shafiy HF, Mashaly MM, Eid MF, Nabeel AI, Fouad R. Synthesis, characterization, and antioxidant/cytotoxic activity of new chromone Schiff base nano-complexes of Zn(II), Cu(II), Ni(II) and Co(II). J. Mol. Struct. 2016; S002228601 6302563–.
DOI: 101016/j.molstruc.2016.03.060.

Peer-review history:
The peer review history for this paper can be accessed here:
https://www.sdiarticle5.com/review-history/88253